© 2016. Published by The Company of Biologists Ltd | Journal of Cell Science (2016) 129, 930-942 doi:10.1242/jcs.172148

RESEARCH ARTICLE

MOBP levels are regulated by Fyn kinase and affect the morphological differentiation of oligodendrocytes

Isabelle Schäfer, Christina Müller, Heiko J. Luhmann and Robin White*

ABSTRACT

Oligodendrocytes are the myelinating glial cells of the central nervous system (CNS). Myelin is formed by extensive wrapping of oligodendroglial processes around axonal segments, which ultimately allows a rapid saltatory conduction of action potentials within the CNS and sustains neuronal health. The non-receptor tyrosine kinase Fyn is an important signaling molecule in oligodendrocytes. It controls the morphological differentiation of oligodendrocytes and is an integrator of axon–glial signaling cascades leading to localized synthesis of myelin basic protein (MBP), which is essential for myelin formation. The abundant myelin-associated oligodendrocytic basic protein (MOBP) resembles MBP in several aspects and has also been reported to be localized as mRNA and translated in the peripheral myelin compartment. The signals initiating local MOBP synthesis are so far unknown and the cellular function of MOBP remains elusive. Here, we show, by several approaches in cultured primary oligodendrocytes, that MOBP synthesis is stimulated by Fyn activity. Moreover, we reveal a new function for MOBP in oligodendroglial morphological differentiation.

KEY WORDS: Oligodendrocyte, Myelin, MOBP, MBP, Fyn, Translational regulation, Morphological differentiation

INTRODUCTION

Oligodendrocytes are the myelinating glial cells of the central nervous system and undergo drastic morphological changes during the differentiation from an oligodendrocyte precursor cell (OPC) to a myelinating oligodendrocyte being capable of recognizing and ensheathing specific axonal segments (Simons and Lyons, 2013). Oligodendroglial maturation and myelination are complex cell biological processes requiring tightly regulated control mechanisms. Several signaling pathways have been described that are required for forming myelin membranes *in vitro* and *in vivo* (Nave and Werner, 2014; White and Krämer-Albers, 2014). Among those, the activation of the oligodendroglial non-receptor tyrosine kinase Fyn has been proposed to be of central importance (Krämer-Albers and White, 2011). Fyn is activated upon axon–glial contact, which is mediated by an interaction of the axonal cell adhesion molecule L1 and axon-associated laminin-2 with an oligodendroglial complex of β1-integrin with contactin-1 (also known as neural cell surface protein F3) (Laursen et al., 2009; White et al., 2008). Furthermore it has been shown that neuronal activity stimulates Fyn kinase in a manner that might be mediated by increased axonal surface expression of L1 (Wake et al., 2011). Recent *in vivo* analyses in zebrafish have confirmed the importance of Fyn for myelin formation supporting previous knockout studies in which Fyn-deficient mice showed hypomyelination in the forebrain (Czopka et al., 2013; Sperber et al., 2001). In oligodendrocytes, Fyn activity appears to control three major downstream pathways affecting the cytoskeleton, morphological differentiation and survival, as well as site-specific control of myelin basic protein (MBP) translation (Krämer-Albers and White, 2011). *Mbp* mRNA is transported from the nucleus to the axon–glial contact site in RNA granules containing a number of RNA-binding proteins, components of the protein synthesis machinery and the small non-coding RNA 715 (sncRNA715), an inhibitor of *Mbp* translation (Bauer et al., 2012; Müller et al., 2013). The central granule protein hnRNP A2 recruits mRNAs containing a specific sequence in their 3′UTR termed the A2 response element (A2RE) which is present in all *Mbp* splice variants (Munro et al., 1999). It has been shown that activated Fyn phosphorylates hnRNP A2 and the granule-associated hnRNP F, stimulating the translation of A2RE-containing mRNAs (White et al., 2008, 2012).

In addition to *Mbp*, other A2RE-containing mRNAs have been proposed to be transported in hnRNP-A2-dependent RNA granules including neuronal CamKIIα (also known as CAMK2A), neurogranin, Arc and oligodendroglial myelin-associated oligodendrocytic basic protein (MOBP) (Barbarese et al., 1999; Gao et al., 2008). There are seven transcript variants of *Mobp* in rats and mice, which are abundantly and exclusively expressed by oligodendrocytes giving rise to small highly basic proteins ranging from ∼10 to ∼20 kDa. They contain a common 68-amino-acid N-terminus and a variable C-terminus (Montague et al., 2006). Like for *Mbp*, A2RE-containing *Mobp* mRNAs (*Mobp*71, *Mobp*81A, *Mobp*99 and *Mobp*169 coding for proteins with 71, 81, 99 and 169 amino acids, respectively) are found in myelin sheath assembly sites and the encoded proteins associate with the major dense line in compact myelin (Gould et al., 1999). The function of MOBP has been associated with the compaction and stabilization of myelin membranes (Gould et al., 2000; Montague et al., 2006). At the cellular level, however, the role of MOBP remains unknown but is likely to be very relevant due to its high abundance. In this study, we addressed the question of whether MOBP synthesis is regulated by Fyn kinase and analyzed whether MOBP knockdown or overexpression affects the morphological differentiation of oligodendrocytes.

RESULTS

Mobp mRNA and protein levels during oligodendrocyte differentiation

The translation of a large number of mRNAs is spatially and temporally controlled and localized mRNAs such as *Mbp* can be detected at least 1 day before the protein is synthesized (Besse and Ephrussi, 2008; Colello et al., 1995). In order to obtain a better understanding of the translational regulation of MOBP, we analyzed *Mobp* mRNA and protein levels in differentiating cultured

Institute of Physiology, University Medical Center of the Johannes Gutenberg University, Duesbergweg 6, Mainz 55128, Germany.

*Author for correspondence (white@uni-mainz.de)

Received 25 March 2015; Accepted 20 January 2016

Journal of Cell Science (2016) 129, 930-942 doi:10.1242/jcs.172148

oligodendrocytes. We isolated OPCs expressing AN2 (also known as CSPG4) from postnatal day (P)9 mice and allowed them to differentiate *in vitro*. Total RNA and protein was isolated after 1, 3, 5 and 7 days *in vitro* (DIV). Reverse transcription and PCR amplification using primers recognizing all *Mbp* and *Mobp* splice variants revealed that *Mobp* and *Mbp* mRNA were already present by 1 DIV (Fig. 1A). As expected, the levels of both *Mobp* and *Mbp* mRNA increased during oligodendrocyte maturation in culture as assessed by RT-qPCR (Fig. 1B). Similar to MBP, MOBP protein can initially be detected in western blots after 5 DIV, whereas the myelin protein 2′,3′-cyclic-nucleotide 3′-phosphodiesterase (CNP) is already present by 3 DIV. The mature oligodendrocyte marker myelin oligodendrocyte glycoprotein (MOG) appeared later than MOBP and MBP (Fig. 1C). In immunostainings, no MOBP and MBP could be detected at 1 DIV and very little reactivity occurred by 3 DIV, whereas at DIV5 both proteins were present in the cytoplasm and cellular processes (Fig. S1). Interestingly, the subcellular distribution of MOBP and MBP was not identical. In contrast to MBP, which is very abundant in the membrane sheets (Aggarwal et al., 2011), MOBP appeared to be more restricted to the

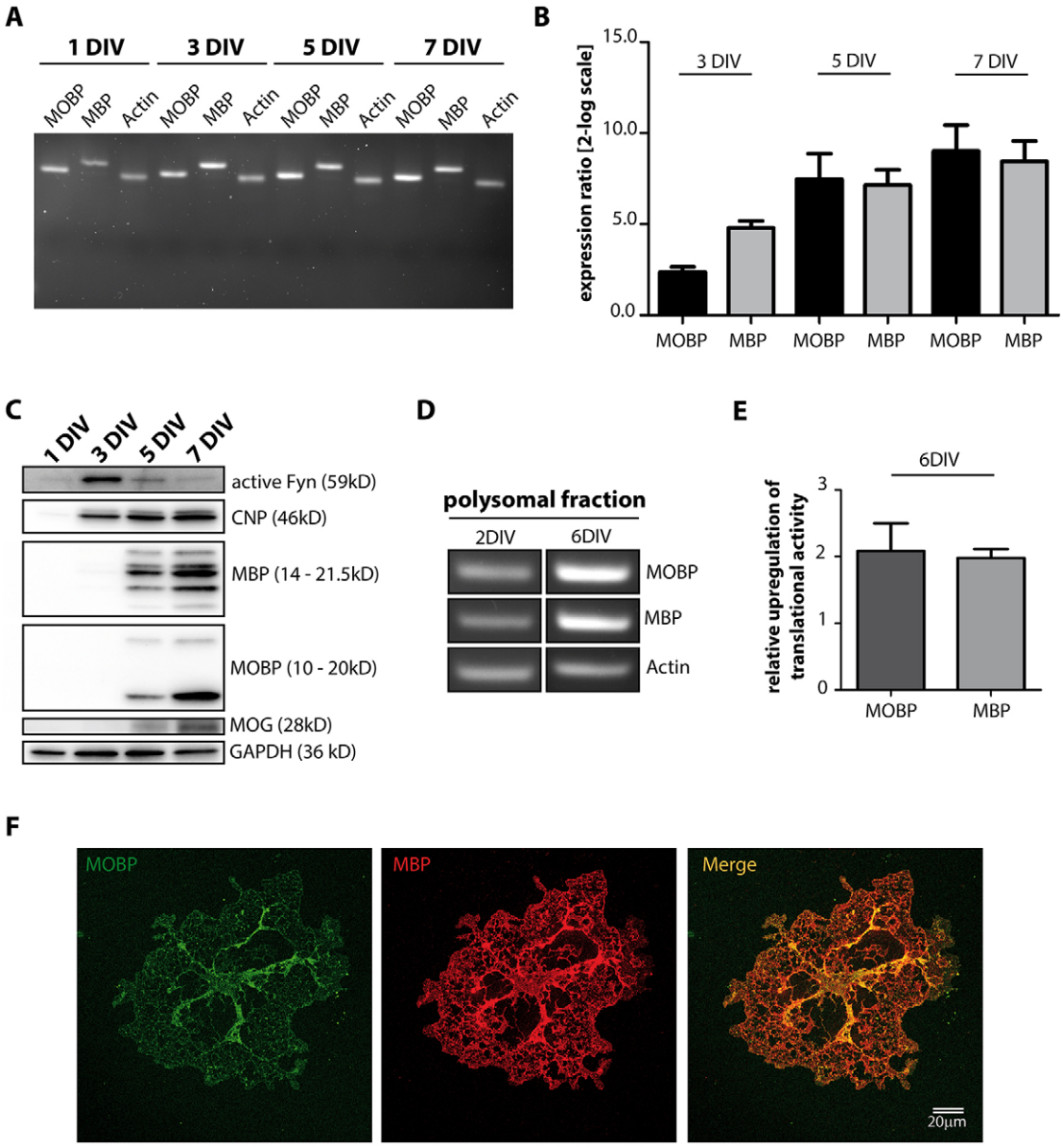

Fig. 1. *Mobp* mRNA and protein levels in differentiating primary oligodendrocytes. (A) Qualitative analysis of *Mobp*, *Mbp* and β-actin mRNA in primary mouse oligodendrocytes cultured *in vitro*. RT-PCR products were analyzed on an ethidium-bromide-stained agarose gel at the indicated time points. (B) Relative quantification of these mRNA levels in differentiating primary oligodendrocytes by qRT-PCR. The results are relative to those at 1 DIV using β-actin as a reference gene. Results are mean±s.e.m. (log2 scale), *n*=3. (C) Detection of active Fyn kinase, CNP, MBP, MOBP and MOG protein in differentiating primary mouse oligodendrocytes as assessed by western blotting at the indicated time points. GAPDH levels were used as a loading control. (D,E) Primary oligodendrocyte lysates (2DIV and 6DIV) were laid on a 10–50% linear sucrose gradient and fractionated by centrifugation. (D) Qualitative analysis of *Mobp*, *Mbp* and β-actin mRNA in primary mouse oligodendrocytes. RT-PCR products were analyzed on an ethidium-bromide-stained agarose gel at the indicated time points. (E) Relative quantification of *Mobp* and *Mbp* mRNA levels in the polysomal fraction of differentiated oligodendrocytes (6 DIV) by qRT-PCR with Rn18S as reference gene and 2 DIV as the reference condition. Results are mean±s.e.m., *n*=2. (F) Immunostaining (a single confocal plane) of MOBP and MBP in a cultured primary oligodendrocyte (5DIV).

Journal of Cell Science (2016) 129, 930-942 doi:10.1242/jcs.172148

oligodendroglial cytoplasm and larger processes (Fig. 1F), supporting previous observations (Montague et al., 1998).

The finding that *Mobp* mRNA can be detected much earlier than MOBP protein could result from different sensitivities of the detection methods used here or by translational repression of *Mobp* during the initial phases of oligodendrocyte differentiation. The latter would suggest a similar control of *Mobp* translation as for *Mbp*. This hypothesis is supported by the finding that *Mobp* mRNA co-immunoprecipitated with hnRNP A2 from cultured primary oligodendrocytes, and is thus associated with the hnRNP-A2-dependent mRNA transport machinery (Fig. S2A,B).

In addition to the proposed model of repressed protein synthesis of *Mobp* and *Mbp* during the early stages of oligodendrocyte differentiation, continuous proteasomal degradation of these proteins could occur in these OPCs. This could also explain why *Mobp* and *Mbp* mRNAs are detectable whereas the proteins are not. To address this possibility, we treated primary mouse OPCs with N-Acetyl-L-leucyl-L-leucyl-L-norleucinal (ALLN), an inhibitor of proteasomal degradation (Kramer-Albers et al., 2006; White et al., 2012). Although tubulin levels increased in ALLN-treated cells, MOBP or MBP protein could not be detected prematurely (Fig. S2C) at this OPC stage. Proteasomal degradation is hence unlikely to delay detection of MOBP and MBP protein.

To support the idea of increased translational activity of *Mobp* and *Mbp* during more mature stages of OPC development, we analyzed the association of *Mobp* and *Mbp* mRNA with polysomes in mature oligodendrocytes (6 DIV) compared to in 2 DIV cultured OPCs by polysome profiling and subsequent analysis of mRNAs associated with the polysomal fraction. There was a strong increase in the amount of *Mobp*, as well as *Mbp*, mRNA associated with the polysomal fraction at 6 DIV compared to 2 DIV (Fig. 1D,E), showing that there was an increase in their translational activity within oligodendrocyte differentiation, further supporting the idea of translational repression during the initial phases of cellular maturation.

In order to understand how translational de-repression occurs in mature oligodendrocytes, we aimed to identify signaling molecules capable of stimulating MOBP protein synthesis.

Fyn kinase activity affects MOBP protein levels

Fyn kinase is highly expressed in differentiating oligodendrocytes (Zhang et al., 2014), is a central integrator of multiple signaling cascades (Krämer-Albers and White, 2011) and induces the translation of *Mbp* (White et al., 2008). As MBP and MOBP expression patterns appear quite similar, we addressed the question of whether Fyn kinase activity also increases MOBP protein levels. In an initial approach, we reduced the levels of Fyn by about 86% by using small interfering RNA (siRNA) and analyzed the resulting changes in MOBP levels (Fig. 2A,B). We analyzed the protein levels of control-siRNA- and Fyn-siRNA-treated cells by western blotting and subsequent densitometric quantification of proteins. The levels of MOBP and MBP were significantly reduced upon Fyn knockdown (reduction of 31% and 29%, respectively), whereas those of proteolipid protein (PLP, also known as PLP1) and CNP did not show a significant change (Fig. 2C–F).

We next investigated whether a change in the activity state of endogenous Fyn kinase during cellular maturation would affect the amount of MOBP. Primary OPCs (1 DIV) were treated with the Src-family kinase inhibitor PP2 (Osterhout et al., 1999) and after 6 days the levels of MOBP, MBP, PLP and CNP were determined by western blotting and densitometric analyses. The application of PP2 resulted in a mean reduction of Fyn activity of 46% (Fig. 3A,C) and led to a significant decrease of MOBP levels by 37% (Fig. 3A,E). As expected, MBP levels were also significantly lower (37%) in PP2-treated cells compared to control cells (Fig. 3A,F), whereas the levels of CNP and PLP were not affected (Fig. 3A,G,H). Application of PP2 at a later stage of oligodendrocyte maturation (5 DIV) also resulted in a prominent reduction of Fyn activity (Fig. 3A,B) and also led to a significant reduction of MOBP levels (Fig. 3A,E) as verified by densitometric analyses of western blots after 2 days of incubation.

In an additional approach, we overexpressed wild-type Fyn (FynWT) or kinase inactive Fyn (control) in primary oligodendrocytes using adeno-associated virus (AAV)-mediated transduction (see Fig. S3A for cellular distribution). The used AAV vectors contain a shortened MBP promoter for efficient expression in oligodendrocytes (von Jonquieres et al., 2013). At 5 days after transduction, cell lysates were analyzed by western blotting and densitometric analyses to determine the relative protein levels of MOBP, MBP, CNP and PLP. To quantify differences in the activity status of Fyn in the different transduction approaches an antibody recognizing active Fyn was used. In the analysis, we assessed the levels of the protein of interest in FynWT-transduced cells relative to those in the kinase-inactive-transduced control cells (Fig. 3E–H). As shown in Fig. 3B and D, the levels of active Fyn were strongly increased in FynWT- compared to kinase-inactive-overexpressing control cells. Furthermore, the protein levels of MOBP and MBP were significantly higher in cells with increased Fyn activity (FynWT, Fig. 3B,E,F), whereas the amounts of PLP and CNP were not significantly different (Fig. 3B,G,H).

In summary, we can show by three independent approaches that the manipulation of Fyn kinase activity affects the protein levels of MOBP and MBP, but not of other myelin proteins, namely PLP and CNP.

Fyn kinase activity stimulates the translation of A2RE-containing *Mobp* mRNAs

We have previously shown that Fyn phosphorylates oligodendroglial hnRNP A2, the trans-acting factor binding to the cis-acting A2RE region in the 3′UTR of *Mbp* mRNA (White et al., 2008). Although all *Mbp* transcript variants include an A2RE, only the *Mobp*71, *Mobp*81A, *Mobp*99 and *Mobp*169 mRNAs contain an A2RE, whereas the *Mobp*69, *Mobp*81B and *Mobp*170 transcripts lack this element (we refer to the rat nomenclature in this manuscript). Having shown a relationship between Fyn activity and endogenous MOBP levels in primary oligodendrocytes, we next used a luciferase-based translational reporter assay to assess whether active Fyn specifically induces the translation of A2RE-containing *Mobp* transcript variants. We cloned the 3′UTR of *Mobp*81A and *Mobp*99, both of which contain an A2RE, as well as the 3′UTR of *Mobp*170, which lacks an A2RE downstream of a firefly luciferase reporter. We co-transfected these constructs either with plasmids coding for kinase-inactive Fyn or for FynWT into Oli-*neu* cells. A plasmid coding for *Renilla* luciferase which is driven by the same promoter as the firefly luciferase (CMV) but lacks downstream regulatory elements was co-transfected in all of the assays. At 2 days after transfection, we lysed the cells and performed a DualGlo luciferase assay (Bauer et al., 2012; White et al., 2008, 2012). We normalized the luminescent firefly relative light units (RLU) to luminescent *Renilla* RLUs to exclude transcriptional contributions in these assays and then compared the relative values from FynWT-transfected cells to those from Fyn-transfected control cells. As shown in Fig. 4A, transfection of FynWT resulted in an increased amount of active Fyn in these experiments. This led to increased translation of the luciferase reporter controlled by the A2RE-containing 3′UTR of *Mobp*81a as

Journal of Cell Science (2016) 129, 930-942 doi:10.1242/jcs.172148

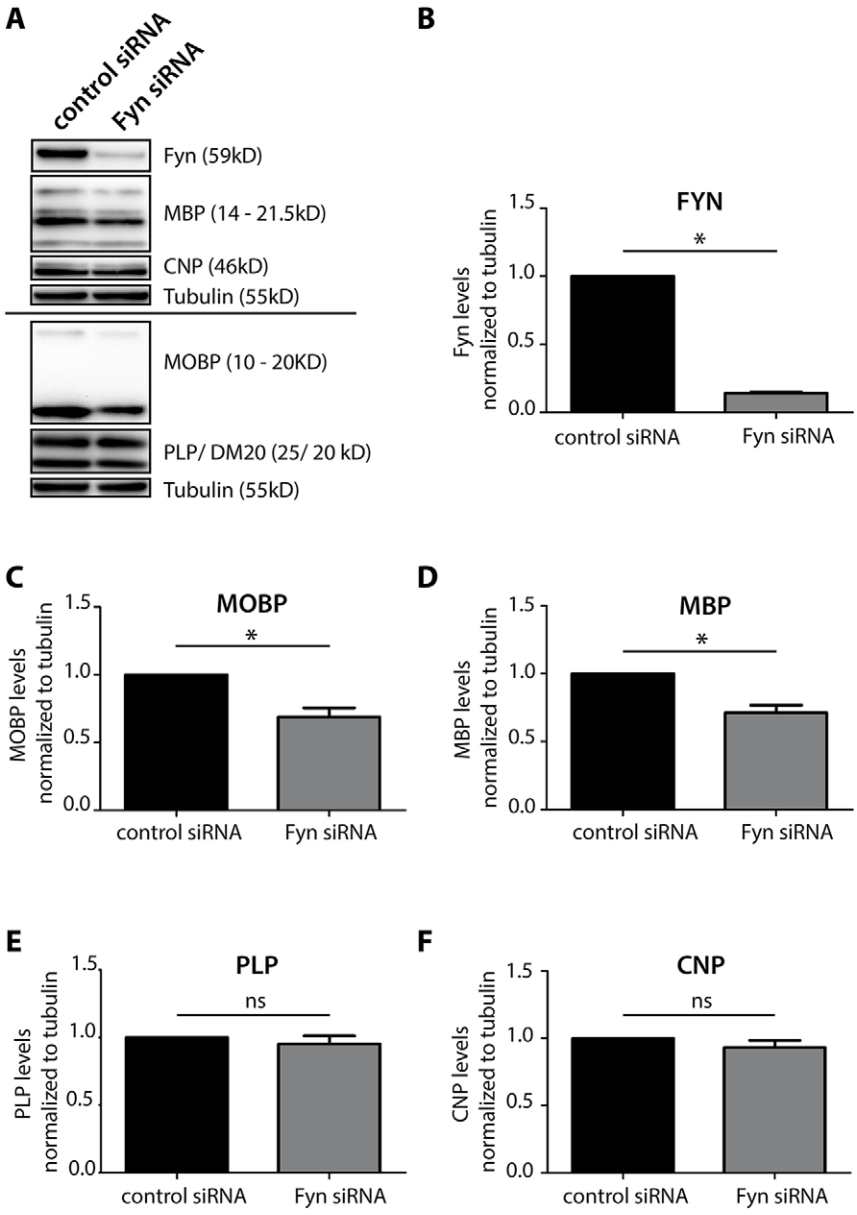

Fig. 2. siRNA-mediated Fyn knockdown results in decreased MOBP levels. Primary mouse oligodendrocytes (5 DIV) were transfected with control or Fyn siRNA and analyzed 48 h later by western blotting. (A) Representative western blots showing detection of Fyn, MBP, CNP, MOBP, PLP and α-tubulin protein in lysates from control- and Fyn-siRNA-treated oligodendrocytes (7 DIV). (B–F) Densitometric analyses of six experiments as depicted in A showing the level of Fyn (B), MOBP (C), MBP (D), PLP (E) and CNP (F) normalized to α-tubulin, and the corresponding value in control transfections. Results are mean±s.e.m., n=6. *P<0.05; ns, not significant (Wilcoxon signed-rank test).

revealed by increased normalized firefly activity in FynWT-transfected Oli-*neu* cells (Fig. 4B). To exclude transcriptional effects by Fyn kinase, we analyzed the luciferase reporter mRNA levels by quantitative real-time PCR (qRT-PCR) and found that they were unaffected by Fyn activity (Fig. 4C). Fyn activity did not increase the normalized luciferase activity and, hence, translation of the *Mobp*170 reporter lacking an A2RE (Fig. 4D) suggesting that there is an A2RE-dependent translational control of MOBP by Fyn kinase. To strengthen this finding, we performed the same luciferase assays with the A2RE-containing 3′UTR of *Mobp*99 mRNA and additionally mutated the A2RE site in this construct (Fig. 4E). As shown in Fig. 4F, increased Fyn activity induced the translation of *Mobp99*, whereas there was no effect on the translation of the *Mobp*99 A2RE mutant.

In conclusion, the experiments in primary oligodendrocytes and the reporter assays in Oli-*neu* cells suggest that active Fyn induces the translation of *Mobp* mRNAs containing an A2RE in their 3′UTR.

Altered MOBP levels affect oligodendroglial morphology

Despite its high abundance, the function of MOBP in oligodendrocytes remains largely unknown on the cellular level. We therefore performed experiments in which we decreased or increased MOBP protein levels in primary oligodendrocytes using small interfering RNA (siRNA)-mediated knockdown or AAV-mediated overexpression, respectively. In these experiments, we observed prominent changes in the cellular morphology (Fig. 5A, upper panel). In order to quantify these, we developed the ‘Fijisurf’ macro for the Fiji software tool together with Biovoxxel (www.biovoxxel.de) to measure the total surface area per cell.

Primary oligodendrocytes were treated with siRNA targeting all *Mobp* transcript variants, which knocked down all MOBP proteins efficiently (Fig. 5B, upper panel). We measured the cell surface area of randomly selected MBP-positive cells and determined a significant decrease of cell surface area in MOBP-siRNA- versus control siRNA-treated cells (Fig. 5A,E). In order to exclude apoptosis-related changes in oligodendroglial morphology

Journal of Cell Science (2016) 129, 930-942 doi:10.1242/jcs.172148

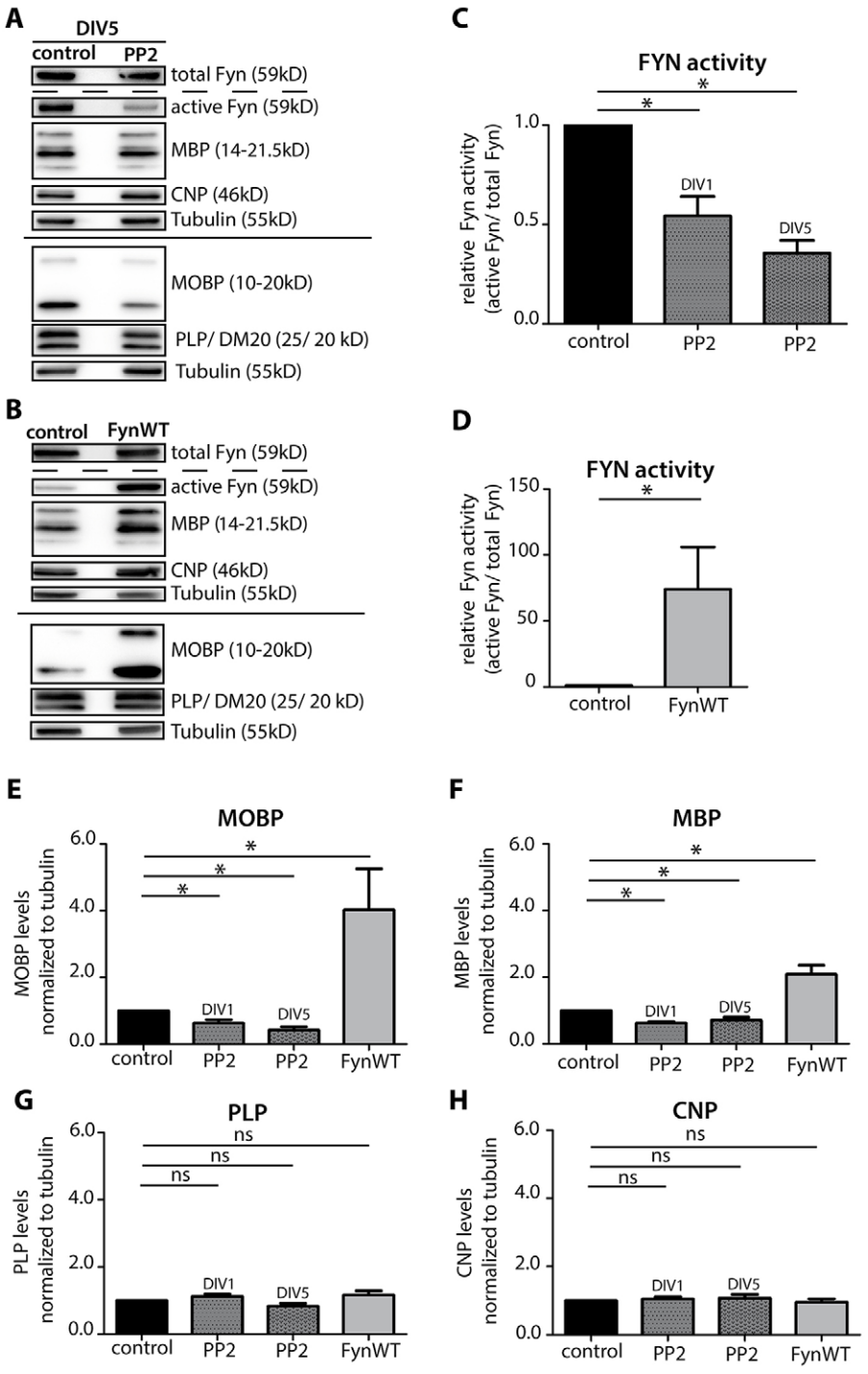

Fig. 3. MOBP levels are affected by the activity status of Fyn. Primary mouse OPCs were treated once with 1 µM PP2 or DMSO (at 1 DIV or 5 DIV) or transduced with AAVs [2×10^9 viral genomes (vg)/ml culture medium] expressing wild-type (FynWT) or kinase-inactive Fyn (control) (at 2 DIV) and analyzed at DIV7 by western blotting. (A) Representative western blots showing detection of total Fyn, active Fyn, MBP, CNP, MOBP, PLP and α-tubulin protein in DMSO- and PP2-treated oligodendrocytes (DIV 5). (B) Representative western blots showing detection of total Fyn, active Fyn, MBP, CNP, MOBP, PLP and α-tubulin protein in oligodendrocytes transduced with FynWT and kinase-inactive Fyn (control). (C–H) Densitometric analyses of experiments as depicted in A and B showing the ratio of active Fyn to total Fyn (C,D), or the levels of MOBP (E), MBP (F), PLP (G) and CNP (H) normalized to α-tubulin, and the corresponding value in DMSO control (n=7) or kinase-inactive control transductions. Results are mean±s.e.m., n=6. *P<0.05; ns, not significant (Wilcoxon signed-rank test).

upon *Mobp* knockdown, we performed fluorimetric TUNEL assays which showed no difference in the relative number of total and apoptotic cells in control or MOBP-siRNA-treated cells (Fig. 5C).

It has been suggested that MBP polymerization affects oligodendroglial membrane extension. As MOBP and MBP have common biophysical properties and could potentially form polymers by heterophilic interactions, we analyzed whether the observed morphological changes could also occur in the absence of MBP. We, therefore, performed the same experimental approach in oligodendrocytes derived from shiverer (*Mbp*^{shi}) mice (Readhead and Hood, 1990). These mice do not express MBP and interestingly show reduced MOBP levels (Fig. S3B–D). We found that untreated *Mbp*^{shi} oligodendrocytes are smaller and that MOBP knockdown in these cells further reduces their cell surface area (Fig. 5A, lower panel; Fig. 5E).

Correspondingly, we transduced primary oligodendrocytes with MOBP-expressing AAVs at 2 DIV to increase their MOBP protein levels prematurely (Fig. 5D). At 5 DIV, we identified MOBP-overexpressing cells by immunocytochemistry and quantified the total MBP-positive surface area per cell in wild-type cells or the total CNP-positive membrane as a proportion of the MBP-positive

Journal of Cell Science (2016) 129, 930-942 doi:10.1242/jcs.172148

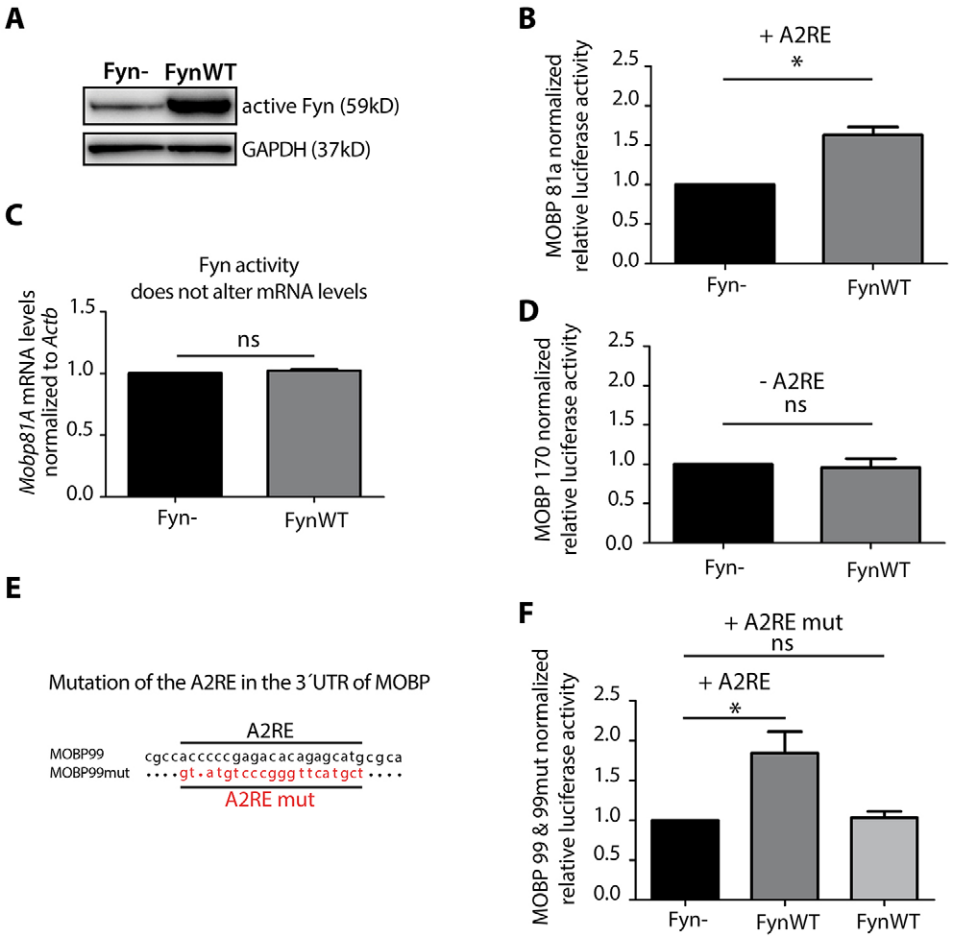

Fig. 4. Fyn-mediated translational regulation of A2RE-containing MOBP reporter constructs. Oli-*neu* cells were co-transfected with kinase-inactive Fyn (Fyn-) or FynWT as well as the indicated MOBP Firefly reporter constructs and DualGlo luciferase assays were performed. (A) Representative western blots with the indicated antibodies showing increased Fyn activity in FynWT-transfected cells. (B) Relative luciferase activity in cells transfected with FynWT compared to those with kinase-inactive Fyn. Activity was assessed by using the A2RE-containing (+ A2RE) MOBP81a reporter and was normalized to the luminescence of co-transfected *Renilla* luciferase. (C) Relative *Mobp81a* mRNA to *Renilla* mRNA levels in cells transfected with kinase-inactive Fyn or FynWT normalized to β-actin mRNA. (D) Relative luciferase activity levels in cells transfected with kinase-inactive Fyn or FynWT. Activity was assessed by using MOBP170 reporter lacking an A2RE (– A2RE) and normalized to the luminescence of co-transfected *Renilla* luciferase. (E) Sequence of the mutated A2RE in the MOBP99mut reporter. (F) Relative luciferase activity in cells transfected with FynWT compared to those with kinase-inactive Fyn as assessed by using the MOBP99 reporter (+A2RE) or the MOBP99mut reporter (+A2RE mut) normalized to the luminescence of co-transfected *Renilla* luciferase. Results are mean±s.e.m., n=9. *P<0.05; ns, not significant (Wilcoxon signed-rank test).

surface area in *Mbp*^{shi} cells (Fig. 5A,E). Relative to eGFP-transduced (control) cells, the overexpression of MOBP81, MOBP169 and MOBP170 resulted in an ∼2-fold increase in the cell surface area in wild-type as well as in *Mbp*^{shi} cells (Fig. 5E). Our findings suggest that MOBP levels affect oligodendroglial morphology in an MBP-independent manner.

To obtain a better insight into the MOBP-induced morphological changes in our experiments, we segmented the cells into somata, myelin-like membranes (sheets) and processes, using the trainable weka segmentation tool for ImageJ (Fig. 6A,B). This allowed us to determine the relative amount of myelin-like membranes per cell. MOBP overexpression resulted in a 2.5-fold increase in the myelin-like membrane fraction compared to in eGFP-transduced control cells (Fig. 6A,C). In contrast, MOBP-siRNA-treated oligodendrocytes contain significantly less myelin-like membranes per cell compared to control-siRNA-treated cells (Fig. 6B,D). Using the Sholl plugin for ImageJ also allowed us to analyze the morphological complexity by quantifying the amount of process branching in these cells. We obtained the number of intersections per given radius in primary oligodendrocytes as illustrated in the colored Sholl profile of the siRNA- or AAV-treated oligodendrocytes (Fig. 6E,F). The complexity of the process meshwork was significantly increased in MOBP-overexpressing cells (Fig. 6G), whereas it was significantly decreased in cells in which MOBP was knocked down (Fig. 6H).

Having shown the effects of MOBP on oligodendroglial morphology, we next intended to analyze this in more detail. We decided to use Oli-*neu* cells which establish a much less complex morphology in respect to process number, length and branching and have successfully been used for the analysis of basic morphological changes previously (Binamé et al., 2013; Gonsior et al., 2014). We transfected plasmids coding for Myc-tagged MOBP71, MOBP169 and MOBP170 as well as eGFP into Oli-*neu* cells and fixed them 2 days later. Cells were immunostained using anti-Myc and anti-NG2 antibodies, and Myc-positive MOBP-transfected cells were analyzed in comparison with eGFP-positive control cells. We used the Fiji freehand line tool to measure the length of the longest process per cell. As shown in Fig. 7A, the processes were approximately 3-fold longer in MOBP-overexpressing cells compared to control cells. Furthermore, we counted the number of all processes per cell and measured the width of the widest process per cell in control and MOBP-overexpressing cells. The overexpression of MOBP71, MOBP169 and MOBP170 significantly increased the number of cellular processes (Fig. 7B) and resulted in cells with significantly wider extensions (Fig. 7C). We deduce that the overexpression of MOBP in Oli-*neu* cells stimulates three major morphological differentiation markers, process length, width and number.

The data obtained in primary oligodendrocytes and Oli-*neu* cells strongly suggest a function of MOBP in the morphological differentiation of oligodendrocytes, which appears to be independent of MBP and is likely to be mediated by the cytoskeleton. Interestingly, MOBP shows a significant colocalization with α-tubulin of 58.3% as determined by confocal microscopy and Mander's correlation coefficient quantification (Fig. S4).

Journal of Cell Science (2016) 129, 930-942 doi:10.1242/jcs.172148

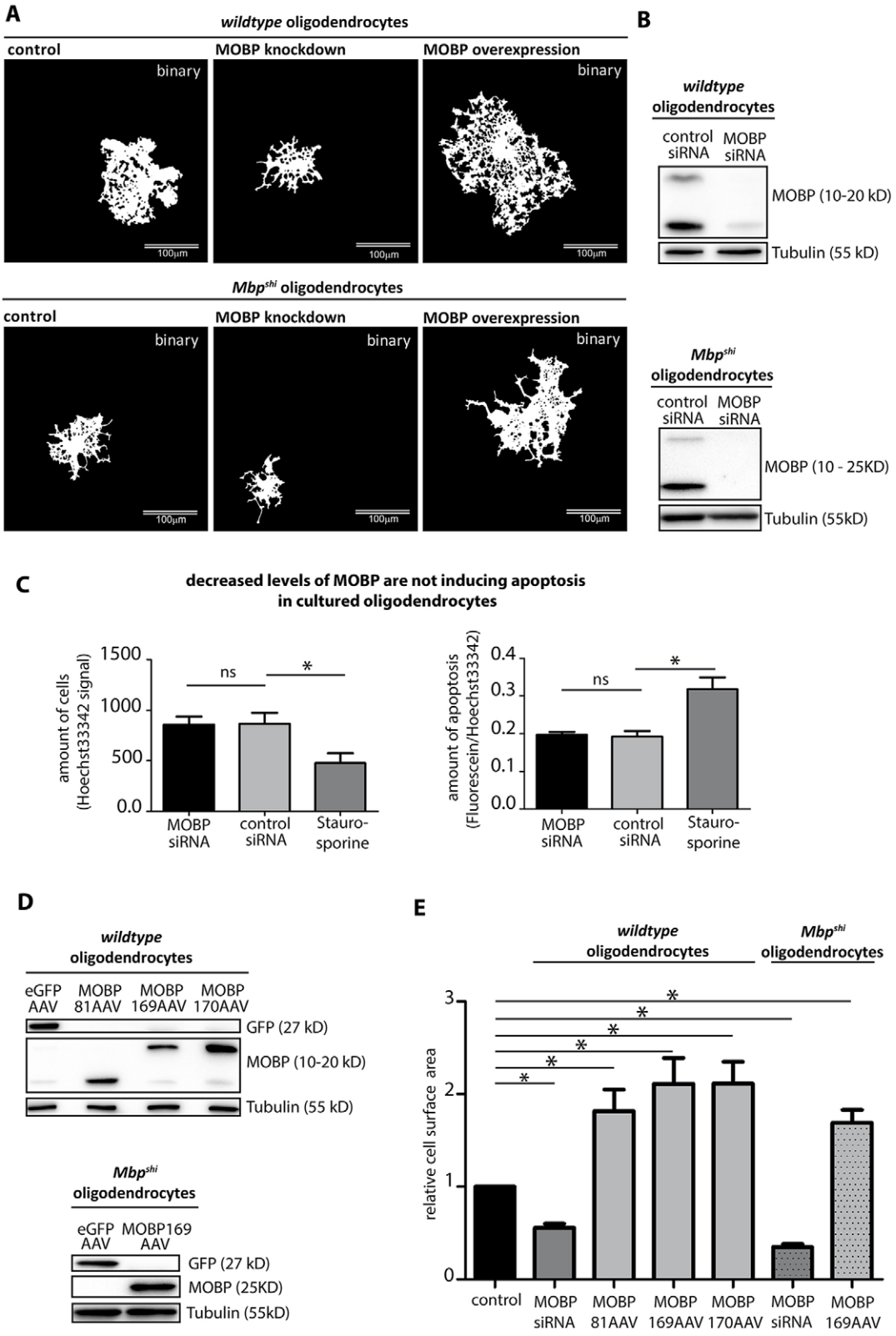

Fig. 5. See next page for legend.

DISCUSSION

The myelination of neuronal axons with distinct functional as well as structural properties requires oligodendrocytes to morphologically respond precisely to these environmental cues. Initially, differentiating oligodendrocyte precursor cells will extend their processes and will either retract them or form stable contacts with axonal targets (Nave and Werner, 2014). These axon–glial contacts will further progress into complex three-dimensional radial

Journal of Cell Science (2016) 129, 930-942 doi:10.1242/jcs.172148

Fig. 5. MOBP affects the cell surface area in primary oligodendrocytes in an MBP-independent manner. MOBP levels were decreased or increased in primary mouse oligodendrocytes derived from wild-type or *Mbp*^{shi} mice (lacking MBP) by siRNA-mediated knockdown or AAV-mediated overexpression, respectively. The total cell surface area was determined using the 'Fijisurf' macro for the Fiji software. (A) Representative binary images of the quantified immunostained total MBP-positive cell surface areas of a control, an MOBP-siRNA-transfected and an MOBP170-AAV-transduced primary wild-type oligodendrocyte (upper panel) or a control, an MOBP–transfected and an MOBP169-AAV-transduced *Mbp*^{shi} oligodendrocyte (lower panel). (B) Representative western blots of control- and MOBP-siRNA-treated primary oligodendrocytes using the indicated antibodies. (C) Control cells were treated with staurosporine, and Fluorimetric TUNEL assays were performed. The relative amount of signal from apoptotic cells (TUNEL positive) as a proportion of the total amount of cells (nuclear staining) was determined and the values were plotted as a percentage of those in untreated control cells. Results are mean±s.e.m., n=4. *P<0.05; ns, not significant (unpaired Student's t-test). (D) Representative western blots of cell lysates form eGFP-AAV- (control), MOBP81-AAV-, MOBP169-AAV- and MOBP170-AAV-transduced primary wild-type oligodendrocytes, or control and MOBP169-AAV-transduced *Mbp*^{shi} oligodendrocytes using the indicated antibodies. (E) Relative cell surface area (compared to control, i.e. control siRNA or eGFP-AAV) in MOBP-deficient or MOBP-overexpressing cells. Results are mean±s.e.m., n=6; *P<0.05 (Wilcoxon signed-rank test).

and lateral ensheathing or wrapping structures, and will finally rest after a certain thickness of the growing myelin sheath has been established (Snaidero et al., 2014). Although the start and especially the stop signals for the ensheathment are only poorly understood, it is known that myelin thickness responds to the axonal diameter (Chomiak and Hu, 2009). Oligodendroglial morphological changes require molecular signaling pathways that can respond to neuronal triggers rapidly and need to be activated or inactivated. One of the concepts to fulfill the aforementioned requirements is the local synthesis of myelin components at the axon–glial contact sites. The reported local Fyn-mediated synthesis of MBP as one of the essential myelin proteins has been proposed to be crucial for myelination (Müller et al., 2013), which is emphasized by the findings that the absence of Fyn or MBP results in a hypomyelinated phenotype in the central nervous system of mice (Readhead and Hood, 1990; Sperber et al., 2001).

Fyn-mediated translation of *Mobp* mRNA

In this study, we present new experimental evidence for Fyn-mediated MBP synthesis and, furthermore, show that Fyn kinase also induces the translation of *Mobp* in oligodendrocytes. It is possible that several mRNAs are transported in oligodendroglial hnRNP-A2-dependent RNA granules, as this has been proposed for other cell types (Carson et al., 2008). It is, however, not so clear whether transported mRNAs are locally translated in response to the same signals. Our results suggest that *MBP* as well as *MOBP* mRNAs are transported in oligodendroglial hnRNP-A2-dependent RNA granules and that the translation of both *Mbp* and *Mobp* is stimulated by Fyn kinase activity. It remains to be shown whether Fyn-stimulated *Mbp* and *Mobp* translation occurs simultaneously or at different time points and/or locations during oligodendroglial development. The immunocytochemical analysis of MOBP and MBP suggests that there is at least a partially differential localization of these two proteins. It seems that MOBP mainly localizes to the larger oligodendroglial processes, whereas MBP can be found additionally in the thin membrane sheets in cultured oligodendrocytes. Interestingly, Fyn kinase can be detected mainly in the larger processes and smaller veins passing through the membrane sheets (Osterhout et al., 1999) allowing the assumption that these are the primary sites of *Mbp* and *Mobp* translation. Subsequently, MBP could be actively or passively moved into the membrane sheets. It has been proposed that the ability of MBP to polymerize is stimulated by structural changes upon contact with the membrane, which could then lead to the formation of a growing protein meshwork that develops into membrane sheets in cultured cells, resembling compact myelin structures *in vivo* (Aggarwal et al., 2011; Bakhti et al., 2014). MBP binds to the membrane in a phosphatidylinositol 4,5-bisphosphate [$PI(4,5)P_2$]-dependent way (Nawaz et al., 2009), but it is not known where exactly MBP initially associates with the membrane and how this is controlled. Fyn is localized in lipid raft membrane microdomains (Krämer et al., 1999) and PI(4,5)P2-enriched lipid rafts have been connected to surface motility (Golub and Caroni, 2005). Hence, MBP could directly associate with PI(4,5)P2 rafts in the plasma membrane upon its Fyn-mediated synthesis, initiating MBP polymerization and membrane sheet extension.

MOBP proteins contain a FYVE (for 'Fab 1, YOTB, Vac 1 and EEA1') domain which is generally postulated to bind specifically to phosphatidylinositol 3-phosphate [PI(3)P] (Stahelin et al., 2014). Interestingly, it has recently been shown for the neuronal protein protrudin, that its FYVE domain binds to other phospholipids including PI(4,5)P2 (Gil et al., 2012). It is possible that newly synthesized MOBP could also associate with PI(4,5)P2-containing lipid rafts. However, the exact mechanisms by which MOBP proteins associate with the plasma membrane remain to be elucidated. It might also be the case that these basic proteins are synthesized near the membrane and further directed to specific cellular locations in their soluble form.

Differential loading of *Mobp* and *Mbp* mRNA into separate hnRNP-A2-dependent granules might be an alternative means to spatio-temporally regulate *Mbp* and *Mobp* localization. A certain degree of remodeling of *Mbp*-containing RNA granules has recently been suggested (Torvund-Jensen et al., 2014) and might include exchanges of targeting molecules. Different subtypes of granules could be directed to distinct cellular locations where they would be translated in response to Fyn kinase activity.

MOBP and oligodendroglial morphological differentiation

Our results also reveal a role of MOBP in morphological differentiation of oligodendrocytes as assessed by the Sholl analysis and, furthermore, in the formation of myelin-like membrane sheets. Our experiments in oligodendrocytes derived from shiverer mice, which lack MBP, suggest that MOBP-mediated morphological impact is independent of MBP. It seems that the presence of MOBP is required to establish a complex architecture of cellular processes in cultured oligodendrocytes. In our experiments, we overexpressed the open reading frames of different *Mobp* variants lacking the 3′UTRs containing regulatory A2RE sequences, thereby focusing on effects mediated at the protein level. Interestingly, the overexpression of the different MOBP isoforms resulted in similar morphological effects both in primary oligodendrocytes as well as in Oli-*neu* cells. It is therefore likely that the function of MOBP in respect to morphological differentiation is mediated by the N-terminal 68 amino acids present in all MOBP isoforms. This common N-terminus contains the above-mentioned cysteine-rich FYVE domain, a Zn^{2+}-binding sequence postulated to mediate membrane binding by hydrophobic interactions, as well as binding of basic residues to negatively charged membrane lipids (Han et al., 2013). The C-termini of the larger MOBP isoforms do not seem to interact with membranes and have been proposed to be located in the small cytoplasmic space of the major dense line in compacted myelin (Myllykoski et al., 2012).

Journal of Cell Science (2016) 129, 930-942 doi:10.1242/jcs.172148

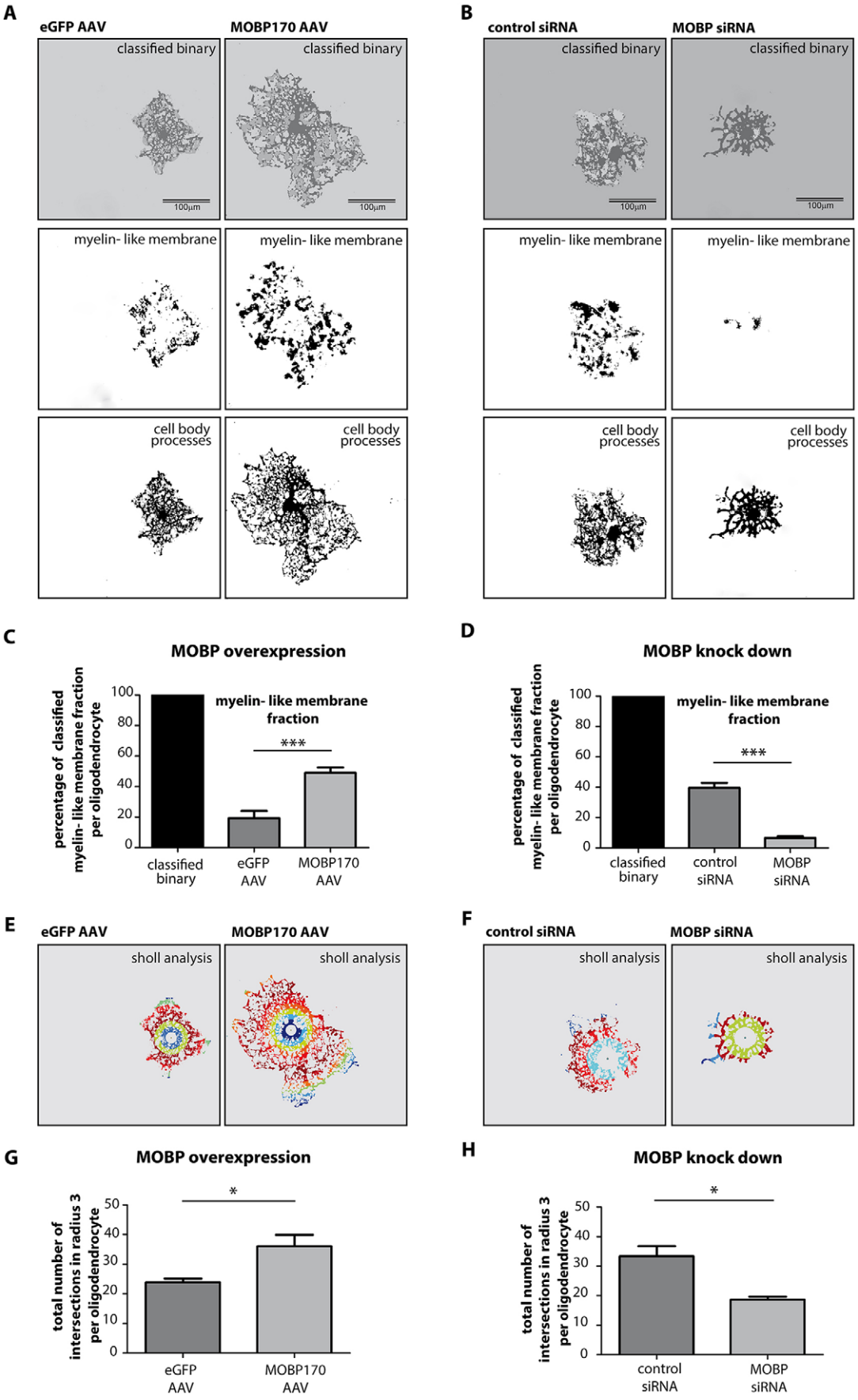

Fig. 6. See next page for legend.

Journal of Cell Science (2016) 129, 930-942 doi:10.1242/jcs.172148

Fig. 6. MOBP increases the percentage of classified myelin-like membrane fraction, as well as the rate of process intersections in primary oligodendrocytes. To classify the myelin-like membrane fraction of the cell surface area in the analyzed oligodendrocytes, the trainable weka segmentation V2.2.1 plugin for ImageJ was used. To obtain the rate of process intersections, the Sholl plugin for ImageJ was used. (A) Classified binary pictures of MOBP-overexpressing and eGFP control cells. (B) Classified binary pictures of oligodendrocytes treated with control and MOBP siRNAs. (C,D) Percentage of classified myelin-like membrane fraction per oligodendrocyte. (E) Sholl profile of MOBP-overexpressing and eGFP control cells. (F) Sholl profile of oligodendrocytes treated with control and MOBP siRNAs. (G,H) Total number of intersections per oligodendrocyte within intersecting radius 3. Results are mean±s.e.m., n=6. *P<0.05; ***P<0.001 (unpaired Student's t-test). Note that the differences in the relative amount of myelin-like membrane in control-siRNA-treated or eGFP-transduced control cells result from different maturation stages in the experimental setups.

Despite the strong morphological effects we observed in oligodendrocytes upon the manipulation of MOBP levels, it is surprising that the absence of MOBP *in vivo* still allows the synthesis of relatively normal myelin (Yamamoto et al., 1999; Yool et al., 2002). However, the absence of MOBP results in an abnormally arranged radial component and the compact myelin appears to be less stable, as exposure to the dysmyelinating hexachlorophene results in a widened major dense line in MOBP-knockout mice (Yamamoto et al., 1999; Yoshikawa, 2001). It has therefore been postulated that MOBP plays a role in the maintenance of compact myelin rather than being required for its synthesis. Our results at the cellular level clearly suggest a function in the developing morphological complexity. It is possible that MOBP actively induces the formation of new processes and stimulates their growth. As oligodendrocytes tend to extend, spread and retract their processes, MOBP could also stabilize newly formed, lengthened or widened processes while counteracting their retraction. Interestingly, an association of MOBP with microtubules has been observed in cultured oligodendrocytes (Montague et al., 1998), and, here, we show a significant colocalization of α-tubulin with MOBP, of ∼58.3%, in primary oligodendrocytes at 5 DIV when the protein synthesis rate of MOBP appears to be strongly enhanced. It is hence likely that our observed changes in morphological differentiation after the manipulation of MOBP levels are at least in part mediated by the interaction of MOBP with the microtubular network. Future studies in myelinating culture systems are required to analyze in more detail whether altered MOBP levels affect the ensheathment and myelination of neuronal axons.

MATERIALS AND METHODS

Cell culture

Oli-*neu* cells (provided by Jacqueline Trotter, University of Mainz, Germany) were regularly tested for contamination and cultured as described previously (White et al., 2012). Primary oligodendrocyte cultures were established from P9 C57BL/6J or C3Fe.SWV-*MBP*^{shi}/J mouse brains by using MACS technology (Miltenyi Biotec). Animal experiments were performed in accordance with the animal policies of the University of Mainz, approved by the German Federal State of Rheinland Pfalz, in accordance with the European Community Council Directive of November 24, 1986 (86_609_EEC). Great care was taken to prevent the animals from suffering. Brain tissue was dissociated using a papain-containing neural tissue dissociation kit and the gentleMACS dissociator (Miltenyi Biotec). Anti-AN2 (NG2) MicroBeads (Miltenyi Biotec) were used to isolate oligodendrocyte precursor cells, which were cultured in poly-L-lysine-coated cell culture vessels in MACS Neuro Medium containing penicillin-streptomycin (100 U/ml), 2 mM L-glutamine and 2% (v/v) NeuroBrew (Miltenyi Biotec) for the indicated time periods.

Antibodies

Monoclonal antibodies were against: CNPase (mouse, 1:500 WB; 1:50 ICC) and α-tubulin (DM1a, mouse, 1:5000 for western blotting), purchased from Sigma-Aldrich; MBP (rat, 1:500 WB; 1:50 ICC), from AbD Serotec; Fyn (mouse, 1:250 for western blotting) from BD Transduction Laboratories. Polyclonal anti-GAPDH (rabbit, 1:5000 for western blotting) was from Bethyl Laboratories; antibody against phosphorylated Src kinase (phosphorylated at Y^{418}) recognizing the autophosphorylated tyrosine residue in activated Src kinase family proteins, including Fyn (rabbit, 1:1000 for western blotting) was from Life Technologies. Antibodies against Myc (mouse 9E10, 1:50 for immunocytochemistry, Claus Pietrzik, University of Mainz, Germany), PLP (rat aa3, 1:10 for western blotting) and AN2 (rat, 1:100 for immunocytochemistry, both Jacqueline Trotter) as well as anti-MOG antibodies (mouse 1:1000 for western blotting, Chris Linington, University of Glasgow, UK) were kindly provided from hybridoma lines. In collaboration with PINEDA antibody service (Berlin) a new MOBP antibody was generated by immunizing rabbits with the NH_2-SQKVAKEGPRLSKNQKFC-$CONH_2$ (18 AS) peptide present in all MOBP isoforms. This antibody was thoroughly tested (data not shown)

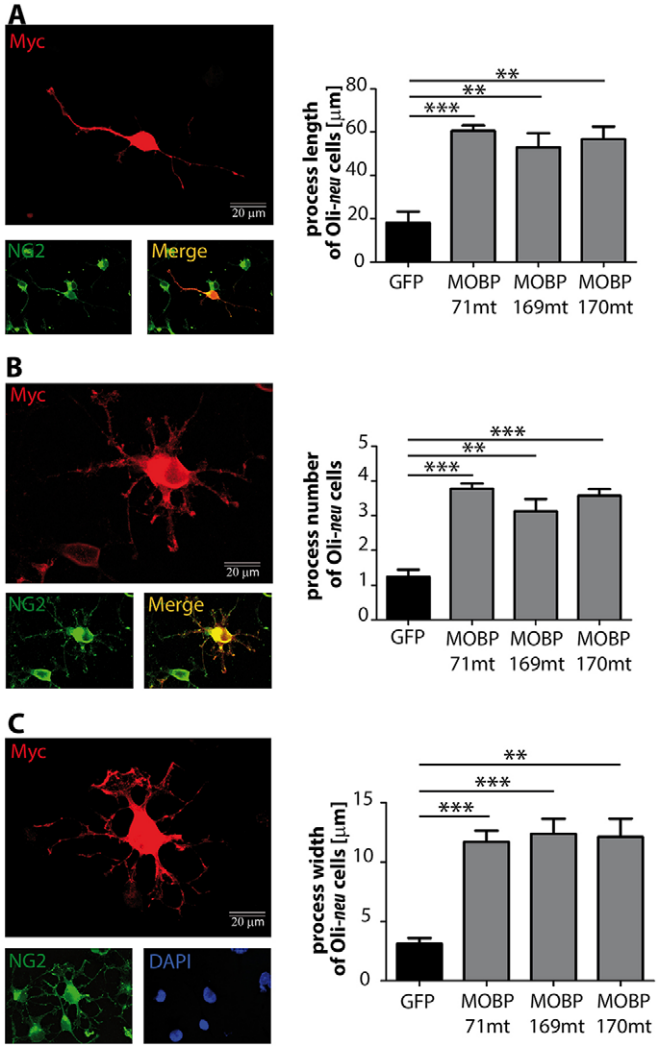

Fig. 7. MOBP overexpression stimulates morphological differentiation of Oli-*neu* cells. Plasmids coding for Myc-tagged (mt) MOBP71, MOBP169 and MOBP170 as well as eGFP were transfected into Oli-*neu* cells and analyzed 2 days later. Myc-positive MOBP-transfected cells were analyzed with the Fiji software tool in respect to three morphological markers, process length (A), number (B) and width (C). Results are mean±s.e.m., n=4. **P<0.01, ***P<0.001 (unpaired Student's t-test).

Journal of Cell Science (2016) 129, 930-942 doi:10.1242/jcs.172148

and used in this study in western blots and for immunocytochemistry (1:20,000 for western blotting; 1:10,000 for immunocytochemistry).

RNA extraction, RT-PCR, qRT-PCR and plasmids

Total RNA from rat brain (P23) was used in cloning of the Firefly reporter constructs and MOBP Myc-tagged constructs as well as total RNA from cultured mouse oligodendrocytes; RNA was isolated using either the miRNeasy Mini Kit (Qiagen) or the RNeasy Mini Kit (Qiagen). mRNA was reverse transcribed using the Transcriptor High Fidelity cDNA Synthesis Kit (Roche Applied Science).

qRT-PCR was performed using the LightCycler TaqMan Master Kit as well as probes and primers designed with the Universal Probe Library in a LightCycler 1.5 System (all Roche Applied Science) or in a StepOnePlus Real-Time PCR System using the TaqMan Fast Advanced Master Mix Kit (all Applied Biosystems). Primer sequences (all in 5′-3′ orientation) of target genes and probes are as follows: *MOBP* (UPL probe #74), GGCTCTCCAAGAACCAGAAG and GCTTGGAGTTGAGGAAGGTG; *MBP* (UPL probe #58), AACATTGTGACACCTCGAACA and TGTCTCTTCCTCCCCAGCTA; Firefly (UPL probe #29), TGAGTACTTCGAAATGTCCGTTC and GTATTCAGCCCATATCGTTTCAT; Renilla (UPL probe #145), GGAGAATAACTTCTTCGTGGAAAC and GCTGCAAATTCTTCTGGTTCTAA; β-actin (UPL probe #106), TGACAGGATGCAGAAGGAGA and CGCTCAGGAGGAGCAATG; glucose-6-phosphate dehydrogenase (G6PDH) (UPL probe #78), GAAAGCAGAGTGAGCCCTTC and CATAGGAATTACGGGCAAAGA; 18S ribosomal RNA (Rn18S): TaqMan Assay ID Mm03928990_g1 (Applied Biosystems). The qRT-PCR crossing points were used for relative quantification based on the $\Delta\Delta C_t$ method using the REST software and β-actin was used as a reference gene (Pfaffl et al., 2002). qRT-PCR products were additionally analyzed using 4% agarose gels stained with ethidium bromide.

Cloning of the *Firefly* reporter constructs or MOBP Myc- and His-tagged constructs expressing the 3′UTRs or open reading frames of different *Mobp* splice variants was performed using standard molecular cloning techniques. Primer sequences (all in 5′-3′ orientation) of target genes are as follows: *MOBP81a*, GCCTCGAATCCCGAGAAGFGGACTTCTCGTG and CGGGCCCTTTTGATCCATCCCCAGGTT; *MOBP99*, GCCTCGAATTCAATGCAATAGAATTTAAAAATG and GCCATCTAGAAATTTAGTAGTTTCTGGTTATTCCCAT; *MOBP170*, GCCTCGAATTCCACCATCTCTTGC and GCCATCTAGACAAACAGAGGGGGTTTAATG; *MOBP71*, GCCTCGAATTCATGAGTCAAAAAGTGG and GCCTCCTCGAGCACAGTCCTGGTC; *MOBP81*, GCCTCGAATTCATGAGTCAAAAAGTGG and GCCTCCTCGAGCTTTTTTCTTGGG; *MOBP169*, GCCTCGAATTCATGAGTCAAAAAGTGG and GCCTCCTCGAGGAACCTAGGAGCT; *MOBP170*, GCCTCGAATTCATGAGTCAAAAAGTGG and GCCTCCTCGAGCCAGAACCTAGGA. Additionally, MOBP Myc- and His-tagged constructs were used as template DNA for cloning of the MOBP-AAV constructs. Primer sequences (all in 5′-3′ orientation) were as follows: MOBP81, GCGAATTCATGAGTCAAAAAGTGG and TATTTTGCGGCCGCTCACTTTTTTCTTGG; MOBP169, GCGAATTCATGAGTCAAAAAGTGG and TATTTTGCGGCCGCTCAGAACCTAGGAG; MOBP170, GCGAATTCATGAGTCAAAAAGTGG and TATTTTGCGGCCGCTTACCAGAACCTAGG.

Firefly luciferase reporter MOBP99 containing the 3′UTR was mutated using the QuikChange Lightning Site-Directed Mutagenesis Kit (Agilent Technologies). Primer sequence (in 5′-3′ orientation) including a SmaI restriction site as follows: MOBP99mut, CCCTCCACGCCGTCATGTCCC GGGTTCATGCTCGCATTAACCC and GGGTTAATGCGAGCATGAACCCGGGACATGACGGCGTGGAGGG.

Luciferase assay

Luciferase assays were performed by using the Dual-Glo Luciferase Assay System (Promega), as described previously (Bauer et al., 2012).

Manipulation of Fyn and MOBP in primary oligodendrocytes

PP2 (Calbiochem, Merck- Millipore) was resuspended in DMSO and added once to the culture medium after 1 DIV or 5 DIV (see Fig. 3) at a concentration of 1 µM in addition to DMSO controls. Wild-type (FynWT), kinase-inactive Fyn, MOBP and eGFP cDNA was cloned downstream of the expression cassette controlled by the shortened MBP promoter, and packaged into AAV vectors as described previously (von Jonquieres et al., 2013). Primary OPCs were transduced with 2×10^9 viral genomes (vg)/ml culture medium after 2 DIV. AAV–eGFP vectors were used as controls. 40 pmol of Fyn siRNA (ON-TARGET plus SMARTpool siRNA, Dharmacon, AGGUGCGAAGUUUCCCAUUA, GCACGUGACUCGUUGUUUC, UAACUGUGGUUUCAUCAAG, CCACGUCAAACAUUAUAAA; all in 5′-3′ orientation) or negative control siRNA (ON-TARGET plus Non-targeting pool, Dharmacon; Allstar Negative control siRNA, Qiagen) were transfected after 5 DIV (and 6 DIV for MOBP siRNA) using Lipofectamine RNAiMax (Life Technologies). Protein levels were analyzed by western blotting after 7 DIV except for the AAV-MOBP-transduced cells, which were analyzed after 5 DIV.

TUNEL assay

Primary mouse oligodendrocytes (5×10^4) were transfected with 40pmol MOBP siRNA or control siRNA using Lipofectamine RNAiMAX Transfection Reagent. As a positive control, cells were treated with 1 µM staurosporine 24 h after transfection (Sigma-Aldrich). After 18 h the relative amount of apoptotic cells and the relative amount of total cells was determined using the DNA Fragmentation Imaging Kit (Roche Applied Science). This is based on a fluorimetric terminal deoxynucleotidyl transferase dUTP nick end labeling (TUNEL) reaction as well as a Hoechst 33342 labeling of nuclei, and was quantified in an Infinite F1000 plate reader (TECAN). The relative values in control siRNA transfections were assessed for MOBP siRNA transfection or to staurosporine treatment.

Inhibition of proteasomal degradation

To inhibit proteasomal degradation, primary oligodendrocytes were treated during differentiation with 100 µM of N-Acetyl-L-leucyl-L-leucyl-L-norleucinal (ALLN) in dimethyl sulfoxide (DMSO) for 4 hours prior to lysis as previously reported (Kramer-Albers et al., 2006; White et al., 2012). Protein levels were analyzed by western blotting.

Western blotting

Cells were lysed in lysis buffer containing 50 mM Tris-HCl, 150 mM NaCl, 1 mM EDTA and 1% Triton X-100 as well as Complete and PhosStop protease and phosphatase inhibitors (Roche Applied Science). Protein samples and molecular mass markers (Biorad or NEB) were separated in 14% SDS-PAGE gels or 4–12% NuPAGE precast gels (Life Technologies) and transferred to PVDF membranes (Roth). Membranes were probed with the indicated antibodies according to standard western blotting procedures and ECL detection, and densitometry analysis was performed in a ChemiDoc XRS+ system and ImageLab software (Biorad).

Immunoprecipitation

For immunoprecipitation of endogenous hnRNP A2, magnetic Protein G Dynabeads (Life Technologies) and anti-hnRNP A2 antibody (EF67, Santa Cruz Biotechnology) were used. After 6 DIV, cultured primary oligodendrocytes were lysed, and 3.2 µg of hnRNP A2 or isotype control anti-FLAG (mouse, Sigma-Aldrich) antibodies were added to 500 µl of lysate and incubated overnight at 4°C under permanent rotation. Then 50 µl Protein G bead slurry per reaction was washed twice with W&B Buffer (sodium phosphate buffer pH 8.0, 0.01% Tween 20) and the antibody–lysate complex was added to the beads and incubated for 2 h at 4°C under permanent rotation. After 10 washing steps with 700 µl lysis buffer, beads were collected in 1 ml ice-cold PBS, separated 1:1 and processed further for protein and RNA analysis by western blotting and RT-PCR, respectively.

Polysomal profiling

Primary mouse oligodendrocytes (4×10^6) were incubated with pre-warmed fresh MACS culture medium containing 100 µg/ml cycloheximide (CHX) at 37°C for 5 min after 2 DIV or 6 DIV. Afterwards, the cells were washed twice on ice with cold PBS containing 100 µg/ml CHX. Cells were lysed for 2 min in lysis buffer containing 30 mM Tris-HCl pH 7.4, 10 mM $MgCl_2$,

100 mM NaCl, 1% (v/v) NP-40, 30 units/ml RNAse inhibitor, EDTA-free protease-inhibitor and 100 µg/ml CHX. Cytosolic lysates were then loaded on top of a previously prepared 10–50% linear sucrose gradient and separated on the gradient for 2 h at 4°C and 217,290 ***g*** in a Optima L-90K centrifuge (Beckmann) with a SW40-Ti rotor. Afterwards, 13 fractions of the same volume were collected, and pooled RNA from polysomal fractions was reverse transcribed. Analysis of association of *Mobp* mRNA, *Mbp* mRNA or actin mRNA with polysomes at the indicated time point was investigated using reverse transcription and qRT-PCR. The qRT-PCR crossing points were used for examination of the relative translation efficiency after 6 DIV compared to after 2 DIV. Rn18S was used as a reference gene. qRT-PCR products were additionally analyzed using 4% agarose gels stained with ethidium bromide.

Immunocytochemistry, microscopy and image analysis

Immunostainings were performed as described previously (White et al., 2012), and images were acquired with an IX81 microscope either with a 20× UPIanFLN (NA=0.50) objective or with a 40× UPIanFLN (NA=0.75) objective, a monochrome fluorescence CCD camera XM10 and the cell^F software (all Olympus) or with an TCS SP5 confocal microscope either with a 40× HCX PL APO CS 1.3 oil objective or a HCX PL APO CS 63×/1.4 oil UV objective connected to a fast resonance scanner and the LAS AF 2.6.3 software (all Leica Microsystems CMS GmbH).

Images were modified and analyzed using Fiji software (Schindelin et al., 2012). Cell surface area measurements of primary oligodendrocytes in pixel^2 were performed using the 'Fijisurf' macro for ImageJ which was developed together with Jan Brocher (Biovoxxel) and can be downloaded at http://www.biovoxxel.de. Ten primary cells per condition were measured for each biological replicate (*n*). To classify the myelin-like membrane (sheet) fraction per cell surface area of the analyzed oligodendrocytes the trainable weka segmentation V2.2.1 plugin for ImageJ was used with the standardized training settings. The rate of process intersections per oligodendrocyte was analyzed by using the Sholl plugin for ImageJ on fragmented binary pictures, representing the process meshwork of the cells with the following settings: starting radius, 10 µm; radius step size, 10 µm; 5 samples per radius; and Sholl method 'intersections'. One representative primary cell per measured biological replicate (*n*) was fragmented and analyzed with the Sholl plugin.

For Oli-*neu* experiments, 20–64 cells were measured per biological replicate (*n*). Process lengths as well as process width were measured using the 'freehand line' tool using the scale bar to define the measured distance in µm. The longest or widest process per cell was measured in each analysis.

The extent of colocalization of MOBP with α-tubulin was measured quantitatively by calculating the Mander's correlation coefficient (MCC), Pearson's correlation coefficient (PCC) and Cost's test for single planes of confocal *z*-stacks using Fiji software with the JACoP plugin as described previously (Bolte and Cordelières, 2006; Manders et al., 1993; Müller et al., 2015). On a randomly selected area of the coverslip one oligodendrocyte was analyzed per biological replicate (*n*). The two different Mander's coefficient values (M1 and M2) describe the independent contributions of two selected channels to the pixels of interest. M1 incorporates the fraction of the red channel (α-tubulin) in regions containing green signal (MOBP), whereas M2 represents the fraction of green channel in regions containing red signals. Here, we focused on the M1 values to show the relative colocalization of α-tubulin with MOBP. MCC values range from 0 to 1 where 0 implies no colocalization (0%) and 1 perfect colocalization (100%). PCC values range from 0 to 1 and the Cost's test gives values for *r* (original), which should be the same as PCC, *r* (randomized), which is supposed to be near 0 for real colocalization, and the *P*-value as percentage, where values higher than 95% mean the colocalization is significant.

Statistical analysis

Data are reported as mean±s.e.m. Student's *t*-test (unpaired) and Wilcoxon signed-rank tests were performed as indicated in the figure legends using GraphPad Prism 5 software. Values of $P<0.05$ were regarded as statistically significant.

Acknowledgements

We thank M. Klugmann, R. Jelinek and B. Lutz for AAV vector preparation, J. Trotter for providing Oli-*neu* cells and other reagents, C. Pietrzik and C. Linington for antibodies, C. Gonsior for help with polysome profiling, M. Hanulova and S. Ritz from IMB Mainz for help with image analysis, as well as N. Knauer for excellent technical assistance.

Competing interests

The authors declare no competing or financial interests.

Author contributions

I.S. designed and performed experiments; C.M performed experiments; I.S. and R.W. analyzed the data and wrote the paper. H.J.L. gave conceptual input; R.W. designed and supervised the study.

Funding

This work was supported by the Deutsche Forschungsgemeinschaft (DFG) [grant number WH168/1-1 to R.W.].

Supplementary information

Supplementary information available online at
http://jcs.biologists.org/lookup/suppl/doi:10.1242/jcs.172148/-/DC1

References

Aggarwal, S., Yurlova, L., Snaidero, N., Reetz, C., Frey, S., Zimmermann, J., Pähler, G., Janshoff, A., Friedrichs, J., Müller, D. J. et al. (2011). A size barrier limits protein diffusion at the cell surface to generate lipid-rich myelin-membrane sheets. *Dev. Cell* **21**, 445-456.

Bakhti, M., Aggarwal, S. and Simons, M. (2014). Myelin architecture: zippering membranes tightly together. *Cell. Mol. Life Sci.* **71**, 1265-1277.

Barbarese, E., Brumwell, C., Kwon, S., Cui, H. and Carson, J. H. (1999). RNA on the road to myelin. *J. Neurocytol.* **28**, 263-270.

Bauer, N. M., Moos, C., van Horssen, J., Witte, M., van der Valk, P., Altenhein, B., Luhmann, H. J. and White, R. (2012). Myelin basic protein synthesis is regulated by small non-coding RNA 715. *EMBO Rep.* **13**, 827-834.

Besse, F. and Ephrussi, A. (2008). Translational control of localized mRNAs: restricting protein synthesis in space and time. *Nat. Rev. Mol. Cell Biol.* **9**, 971-980.

Binamé, F., Sakry, D., Dimou, L., Jolivel, V. and Trotter, J. (2013). NG2 regulates directional migration of oligodendrocyte precursor cells via Rho GTPases and polarity complex proteins. *J. Neurosci.* **33**, 10858-10874.

Bolte, S. and Cordelières, F. P. (2006). A guided tour into subcellular colocalization analysis in light microscopy. *J. Microsc.* **224**, 213-232.

Carson, J. H., Gao, Y., Tatavarty, V., Levin, M. K., Korza, G., Francone, V. P., Kosturko, L. D., Maggipinto, M. J. and Barbarese, E. (2008). Multiplexed RNA trafficking in oligodendrocytes and neurons. *Biochim. Biophys. Acta* **1779**, 453-458.

Chomiak, T. and Hu, B. (2009). What is the optimal value of the g-ratio for myelinated fibers in the rat CNS? A theoretical approach. *PLoS ONE* **4**, e7754.

Colello, R. J., Devey, L. R., Imperato, E. and Pott, U. (1995). The chronology of oligodendrocyte differentiation in the rat optic nerve: evidence for a signaling step initiating myelination in the CNS. *J. Neurosci.* **15**, 7665-7672.

Czopka, T., ffrench-Constant, C. and Lyons, D. A. (2013). Individual oligodendrocytes have only a few hours in which to generate new myelin sheaths in vivo. *Dev. Cell* **25**, 599-609.

Gao, Y., Tatavarty, V., Korza, G., Levin, M. K. and Carson, J. H. (2008). Multiplexed dendritic targeting of alpha calcium calmodulin-dependent protein kinase II, neurogranin, and activity-regulated cytoskeleton-associated protein RNAs by the A2 pathway. *Mol. Biol. Cell* **19**, 2311-2327.

Gil, J.-E., Kim, E., Kim, I.-S., Ku, B., Park, W. S., Oh, B. H., Ryu, S. H., Cho, W. and Heo, W. D. (2012). Phosphoinositides differentially regulate protrudin localization through the FYVE domain. *J. Biol. Chem.* **287**, 41268-41276.

Golub, T. and Caroni, P. (2005). PI(4,5)P2-dependent microdomain assemblies capture microtubules to promote and control leading edge motility. *J. Cell Biol.* **169**, 151-165.

Gonsior, C., Binamé, F., Frühbeis, C., Bauer, N. M., Hoch-Kraft, P., Luhmann, H. J., Trotter, J. and White, R. (2014). Oligodendroglial p130Cas is a target of Fyn kinase involved in process formation, cell migration and survival. *PLoS ONE* **9**, e89423.

Gould, R. M., Freund, C. M. and Barbarese, E. (1999). Myelin-associated oligodendrocytic basic protein mRNAs reside at different subcellular locations. *J. Neurochem.* **73**, 1913-1924.

Gould, R. M., Freund, C. M., Palmer, F. and Feinstein, D. L. (2000). Messenger RNAs located in myelin sheath assembly sites. *J. Neurochem.* **75**, 1834-1844.

Han, H., Myllykoski, M., Ruskamo, S., Wang, C. and Kursula, P. (2013). Myelin-specific proteins: a structurally diverse group of membrane-interacting molecules. *BioFactors* **39**, 233-241.

Krämer, E.-M., Klein, C., Koch, T., Boytinck, M. and Trotter, J. (1999). Compartmentation of Fyn kinase with glycosylphosphatidylinositol-anchored molecules in oligodendrocytes facilitates kinase activation during myelination. *J. Biol. Chem.* **274**, 29042-29049.

Krämer-Albers, E.-M. and White, R. (2011). From axon–glial signalling to myelination: the integrating role of oligodendroglial Fyn kinase. *Cell. Mol. Life Sci.* **68**, 2003-2012.

Kramer-Albers, E.-M., Gehrig-Burger, K., Thiele, C., Trotter, J. and Nave, K.-A. (2006). Perturbed interactions of mutant proteolipid protein/DM20 with cholesterol and lipid rafts in oligodendroglia: implications for dysmyelination in spastic paraplegia. *J. Neurosci.* **26**, 11743-11752.

Laursen, L. S., Chan, C. W. and ffrench-Constant, C. (2009). An integrin-contactin complex regulates CNS myelination by differential Fyn phosphorylation. *J. Neurosci.* **29**, 9174-9185.

Manders, E. M. M., Verbeek, F. J. and Aten, J. A. (1993). Measurement of co-localization of objects in dual-colour confocal images. *J. Microscopy* **169**, 375-382.

Montague, P., Barrie, J. A., Thomson, C. E., Kirkham, D., McCallion, A. S., Davies, R. W., Kennedy, P. G. and Griffths, I. R. (1998). Cytoskeletal and nuclear localization of myelin oligodendrocytic basic protein isoforms. *Eur. J. Neurosci.* **10**, 1321-1328.

Montague, P., McCallion, A. S., Davies, R. W. and Griffiths, I. R. (2006). Myelin-associated oligodendrocytic basic protein: a family of abundant CNS myelin proteins in search of a function. *Dev. Neurosci.* **28**, 479-487.

Müller, C., Bauer, N. M., Schäfer, I. and White, R. (2013). Making myelin basic protein – from mRNA transport to localized translation. *Front. Cell. Neurosci.* **7**, 169.

Müller, C., Schäfer, I., Luhmann, H. J. and White, R. (2015). Oligodendroglial Argonaute protein Ago2 associates with molecules of the Mbp mRNA localization machinery and is a downstream target of Fyn kinase. *Front. Cell. Neurosci.* **9**, 431.

Munro, T. P., Magee, R. J., Kidd, G. J., Carson, J. H., Barbarese, E., Smith, L. M. and Smith, R. (1999). Mutational analysis of a heterogeneous nuclear ribonucleoprotein A2 response element for RNA trafficking. *J. Biol. Chem.* **274**, 34389-34395.

Myllykoski, M., Baumgärtel, P. and Kursula, P. (2012). Conformations of peptides derived from myelin-specific proteins in membrane-mimetic conditions probed by synchrotron radiation CD spectroscopy. *Amino Acids* **42**, 1467-1474.

Nave, K.-A. and Werner, H. B. (2014). Myelination of the nervous system: mechanisms and functions. *Annu. Rev. Cell Dev. Biol.* **30**, 503-533.

Nawaz, S., Kippert, A., Saab, A. S., Werner, H. B., Lang, T., Nave, K.-A. and Simons, M. (2009). Phosphatidylinositol 4,5-bisphosphate-dependent interaction of myelin basic protein with the plasma membrane in oligodendroglial cells and its rapid perturbation by elevated calcium. *J. Neurosci.* **29**, 4794-4807.

Osterhout, D. J., Wolven, A., Wolf, R. M., Resh, M. D. and Chao, M. V. (1999). Morphological differentiation of oligodendrocytes requires activation of Fyn tyrosine kinase. *J. Cell Biol.* **145**, 1209-1218.

Pfaffl, M. W., Horgan, G. W. and Dempfle, L. (2002). Relative expression software tool (REST(C)) for group-wise comparison and statistical analysis of relative expression results in real-time PCR. *Nucleic Acids Res.* **30**, e36.

Readhead, C. and Hood, L. (1990). The dysmyelinating mouse mutations shiverer (shi) and myelin deficient (shimld). *Behav. Genet.* **20**, 213-234.

Schindelin, J., Arganda-Carreras, I., Frise, E., Kaynig, V., Longair, M., Pietzsch, T., Preibisch, S., Rueden, C., Saalfeld, S., Schmid, B. et al. (2012). Fiji: an open-source platform for biological-image analysis. *Nat. Methods* **9**, 676-682.

Simons, M. and Lyons, D. A. (2013). Axonal selection and myelin sheath generation in the central nervous system. *Curr. Opin. Cell Biol.* **25**, 512-519.

Snaidero, N., Möbius, W., Czopka, T., Hekking, L. H. P., Mathisen, C., Verkleij, D., Goebbels, S., Edgar, J., Merkler, D., Lyons, D. A. et al. (2014). Myelin membrane wrapping of CNS axons by PI(3,4,5)P3-dependent polarized growth at the inner tongue. *Cell* **156**, 277-290.

Sperber, B. R., Boyle-Walsh, E. A., Engleka, M. J., Gadue, P., Peterson, A. C., Stein, P. L., Scherer, S. S. and McMorris, F. A. (2001). A unique role for Fyn in CNS myelination. *J. Neurosci.* **21**, 2039-2047.

Stahelin, R. V., Scott, J. L. and Frick, C. T. (2014). Cellular and molecular interactions of phosphoinositides and peripheral proteins. *Chem. Phys. Lipids* **182**, 3-18.

Torvund-Jensen, J., Steengaard, J., Reimer, L., Fihl, L. B. and Laursen, L. S. (2014). Transport and translation of MBP mRNA is regulated differently by distinct hnRNP proteins. *J. Cell Sci.* **127**, 1550-1564.

von Jonquieres, G., Mersmann, N., Klugmann, C. B., Harasta, A. E., Lutz, B., Teahan, O., da Housley, G., Fröhlich, D., Krämer-Albers, E. M. and Klugmann, M. (2013). Glial promoter selectivity following AAV-delivery to the immature brain. *PLoS ONE* **8**, e65646.

Wake, H., Lee, P. R. and Fields, R. D. (2011). Control of local protein synthesis and initial events in myelination by action potentials. *Science* **333**, 1647-1651.

White, R. and Krämer-Albers, E.-M. (2014). Axon-glia interaction and membrane traffic in myelin formation. *Front. Cell. Neurosci.* **7**, 284.

White, R., Gonsior, C., Kramer-Albers, E.-M., Stohr, N., Huttelmaier, S. and Trotter, J. (2008). Activation of oligodendroglial Fyn kinase enhances translation of mRNAs transported in hnRNP A2-dependent RNA granules. *J. Cell Biol.* **181**, 579-586.

White, R., Gonsior, C., Bauer, N. M., Krämer-Albers, E.-M., Luhmann, H. J. and Trotter, J. (2012). Heterogeneous nuclear ribonucleoprotein (hnRNP) F is a novel component of oligodendroglial RNA transport granules contributing to regulation of myelin basic protein (MBP) synthesis. *J. Biol. Chem.* **287**, 1742-1754.

Yamamoto, Y., Yoshikawa, H., Nagano, S., Kondoh, G., Sadahiro, S., Gotow, T., Yanagihara, T. and Sakoda Saburo (1999). Myelin-associated oligodendrocytic basic protein is essential for normal arrangement of the radial component in central nervous system myelin. *Eur. J. Neurosci.* **11**, 847-855.

Yool, D., Montague, P., McLaughlin, M., McCulloch, M. C., Edgar, J. M., Nave, K.-A., Davies, R. W., Griffiths, I. R. and McCallion, A. S. (2002). Phenotypic analysis of mice deficient in the major myelin protein MOBP, and evidence for a novel Mobp isoform. *Glia* **39**, 256-267.

Yoshikawa, H. (2001). Myelin-associated oligodendrocytic basic protein modulates the arrangement of radial growth of the axon and the radial component of myelin. *Med. Electron Microsc.* **34**, 160-164.

Zhang, Y., Chen, K., Sloan, S. A., Bennett, M. L., Scholze, A. R., O'Keeffe, S., Phatnani, H. P., Guarnieri, P., Caneda, C., Ruderisch, N. et al. (2014). An RNA-sequencing transcriptome and splicing database of glia, neurons, and vascular cells of the cerebral cortex. *J. Neurosci.* **34**, 11929-11947.